Constraints on the unified model of dark matter and dark energy*

Lü Jian-Bo(吕剑波)[a)†], Wu Ya-Bo(吴亚波)[a)],
Xu Li-Xin(徐立昕)[b)], and Wang Yu-Ting(王钰婷)[b)]

[a)] *Department of Physics, Liaoning Normal University, Dalian* 116029, *China*

[b)] *School of Physics and Optoelectronic Technology, Dalian University of Technology, Dalian* 116024, *China*

(Received 4 December 2010; revised manuscript received 22 February 2011)

Using recently observed data: the Constitution dataset of type supernovae Ia (SNIa), the observational Hubble data (OHD), the measurement results of baryon acoustic oscillation (BAO) from the Sloan Digital Sky Survey (SDSS) and the Two Degree Field Galaxy Redshift Survey (2dFGRS), and the current cosmic microwave background (CMB) data from the five-year Wilkinson Microwave Anisotropy Probe (WMAP), we apply the Markov Chain Monte Carlo method to investigate the observational constraints on the generalized Chaplygin gas (GCG) model as the unification of dark matter and dark energy. For this unified model, the constraints on GCG mixture are discussed by considering the different expressions of current matter density or considering constraints as being independent of the matter quantity $\Omega_{\rm m}$.

Keywords: generalized Chaplygin gas, unification of dark matter and dark energy

PACS: 98.80.–k **DOI:** 10.1088/1674-1056/20/7/079801

1. Introduction

Since 1998, type Ia supernova (SNIa) observations[1] have shown that our universe has entered into a phase of accelerating expansion. During the years from that time, many additional observational results, including current cosmic microwave background (CMB) anisotropy measurement[2] and the data of the large scale structure (LSS),[3] also strongly support this suggestion. These cosmic observations indicate that the baryon matter component is about 5% of the total energy density, and about 95% energy density in universe is invisible. Considering the four-dimensional standard cosmology, this accelerated expansion of the universe predicts that dark energy (DE), as an exotic component with negative pressure, fills the universe. It is shown that DE takes up about two-thirds of the total energy density from cosmic observations. In addition, theoretical DE models have already been constructed.[4−13] In these models, the generalized Chaplygin gas (GCG) model has been widely studied for interpreting the accelerating universe.[14−17] The most interesting property for this scenario is that two unknown dark sections in universe dark energy and dark matter can be unified by using an exotic equation of state. In this paper, we use the Markov Chain Monte Carlo (MCMC) technique to constrain the GCG model from recently observed data: the Constitution dataset[18] including 397 type Ia supernovae, the observational Hubble data (OHD),[19] the observed results of baryon acoustic oscillation (BAO) from the Sloan Digital Sky Survey (SDSS) and the Two Degree Field Galaxy Redshift Survey (2dFGRS),[20,21] and the five-year Wilkinson Microwave Anisotropy Probe (WMAP) results for cosmic microwave background measurement.[22]

2. Model and analysis method

We consider an exotic background fluid, dubbed as GCG, with the following equation of state:[15]

$$p_{\rm GCG} = -\frac{A}{\rho^{\alpha}_{\rm GCG}}, \tag{1}$$

where $\rho_{\rm GCG}$ and $p_{\rm GCG}$ are energy density and pressure for the GCG fluid, A and α are parameters in the model. The GCG model can be interpreted as an entangled mixture of dark matter and dark energy, since both components interact within a single fluid. Detailedly, by using the energy conservation equation in the Friedmann–Robertson–Walker cosmology, $\mathrm{d}(\rho a^3) = -p\mathrm{d}(a^3)$, the energy density of GCG fluid

*Project supported by the National Natural Science Foundation of China (Grant Nos. 10875056 and 10703001) and the Specialized Research Fund for the Doctoral Program of Higher Education of China (Grant No. 20070141034).

†Corresponding author. E-mail: lvjianbo819@163.com

© 2011 Chinese Physical Society and IOP Publishing Ltd

is obtained as follows:

$$\rho_{\rm GCG} = \rho_{0\rm GCG}\left[A_{\rm s}+(1-A_{\rm s})(1+z)^{3(1+\alpha)}\right]^{1/(1+\alpha)}, \quad (2)$$

where $A_{\rm s} = A/\rho_{0\rm GCG}^{1+\alpha}$, z denotes the redshift with the relation $1+z = 1/a$ (a is the scale factor of universe). From Eq. (2) one can see that the GCG fluid behaves as dust at an early stage and as a dark energy at a later stage, then it is often considered to be the unification of dark matter and dark energy. If we consider that the universe is filled with three components — the GCG component, the baryon matter component and the radiation component, one has the total energy density $\rho_{\rm total} = \rho_{\rm GCG} + \rho_{\rm b} + \rho_{\rm r}$. Making use of the Friedmann equation, the Hubble parameter H is expressed as

$$\begin{aligned} H^2 &= \frac{8\pi G\rho_{\rm total}}{3} \\ &= H_0^2\{(1-\Omega_{\rm b}-\Omega_{\rm r}) \\ &\quad \times [A_{\rm s}+(1-A_{\rm s})(1+z)^{3(1+\alpha)}]^{1/(1+\alpha)} \\ &\quad + \Omega_{\rm b}(1+z)^3 + \Omega_{\rm r}(1+z)^4\}, \end{aligned} \quad (3)$$

where $H_0 = 100$ h $(\rm km\cdot s^{-1}\cdot Mpc^{-1})$ is the current Hubble constant, $\Omega_{\rm b}$ and $\Omega_{\rm r}$ denote the dimensionless baryon matter and radiation densities, respectively. In what follows, we perform a global fitting on determining the GCG model parameters using the MCMC approach. Here, since the GCG fluid is considered to be the unified model of dark matter and dark energy, the dark matter density parameter is not included in the background equation (3). Thus, we investigate the constraint on the GCG mixture by using the different expressions of current matter density or considering the constraint being independent of the quantity $\Omega_{\rm m}$. In our analysis, the MCMC code is listed in the publicly available CosmoMC package,[23] which has been modified to include the new model parameters $A_{\rm s}$ and α. In the calculation, the baryon matter density is taken to be varied with a tophat prior: $\Omega_{\rm b}h^2 \in [0.005, 0.1]$. In addition, for each MCMC calculation on GCG model in the following part, we run 8 independent chains. To obtain converged results, we test the convergence of the chains by typically setting $R-1$ to be less than 0.03.

3. Discussion for constraint on the unified model of dark matter and dark energy

For Gaussian distributed analysis, the likelihood function is written as $L \propto {\rm e}^{-\chi^2/2}$. We consider a total χ^2

$$\chi^2_{\rm total} = \chi^2_{\rm SNIa} + \chi^2_{\rm OHD} + \chi^2_{\rm BAO} + \chi^2_{\rm CMB}, \quad (4)$$

where the separate likelihoods of SNIa, OHD, BAO and CMB are given by Eqs. (A5), (A7), (A15) and (A21) in Appendix A. The constraint method and the dataset used in this paper are presented in Appendix A. From the expressions of $\chi^2_{\rm BAO}$ and $\chi^2_{\rm CMB}$, we can see that they are related with the matter density $\Omega_{\rm m}$. According to Eq. (2), by considering that the universe is dominated by the matter component at high redshift ($z \gg 1$), i.e., relative to the dark matter density the dark energy density is negligible, one can obtain an effective expression of the current matter density, $\Omega_{\rm m} = \Omega_{\rm b}+(1-\Omega_{\rm b}-\Omega_{\rm r})(1-A_{\rm s})^{1/(1+\alpha)}$.[24–26] In Fig. 1(a), we show one-dimensional (1D) probability distribution of each parameter and two-dimensional (2D) plots for parameters between each other in the GCG model.

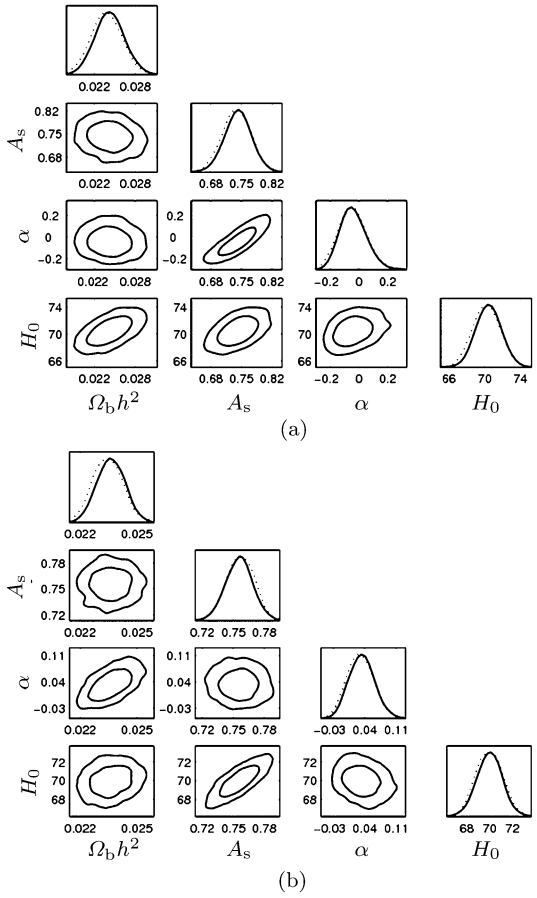


Fig. 1. The 1D constraints on individual parameters: $\Omega_{\rm b}h^2, A_{\rm s}, \alpha, H_0$ and 2D contours on these parameters with 1σ and 2σ confidence levels between each other, where the total χ^2 expression, Eq.(4), is used in the calculation, with effective expression of the current matter density (a) $\Omega_{\rm m} = \Omega_{\rm b} + \left(1-\Omega_{\rm b}-\Omega_{\rm r}\right)(1-A_{\rm s})^{1/(1+\alpha)}$, and (b) $\Omega_{\rm m} = 1-\Omega_{\rm r}-A_{\rm s}(1-\Omega_{\rm b}-\Omega_{\rm r})$.

Dotted lines are mean likelihoods of samples, and solid lines are marginalized probabilities for 1D distribution in the figure. In addition, in several papers someone also takes a form, $\Omega_{\rm m} = 1-\Omega_{\rm r}-A_{\rm s}(1-\Omega_{\rm b}-\Omega_{\rm r})$,[27–29]

Table 1. The data fitting results of GCG model parameters with 1σ and 2σ confidence levels.

Parameter	$\Omega_{\rm m}=\Omega_{\rm b}+\big(1-\Omega_{\rm b}-\Omega_{\rm r}\big)(1-A_{\rm s})^{1/(1+\alpha)}$	$\Omega_{\rm m}=1-\Omega_{\rm r}-A_{\rm s}(1-\Omega_{\rm b}-\Omega_{\rm r})$
$\Omega_{\rm b}h^2$	$0.0240^{+0.0043+0.0059}_{-0.0045-0.0063}$	$0.0234^{+0.0016+0.0022}_{-0.0014-0.0018}$
$A_{\rm s}$	$0.740^{+0.061+0.084}_{-0.062-0.088}$	$0.759^{+0.024+0.032}_{-0.028-0.040}$
α	$-0.056^{+0.209+0.304}_{-0.165-0.209}$	$0.028^{+0.062+0.087}_{-0.049-0.070}$
H_0	$70.35^{+2.89+4.07}_{-2.99-4.09}$	$70.11^{+2.05+3.12}_{-2.31-3.07}$
$\chi^2_{\rm min}(\chi^2_{\rm min}/{\rm dof})$	478.022(1.157)	477.370(1.156)

dof represents the degree of freedom.

which is related to ΛCDM model, i.e., the GCG is taken as a mixture of interacting dark matter and a cosmological constant-type dark energy. Following this expression, the confidence regions of the GCG model parameters are plotted in Fig. 1(b). According to Fig. 1, for these two cases the constraint results on the best fit values of parameters with 1σ and 2σ confidence levels are listed in Table 1. For these two cases, the total χ^2 expression, Eq. (4), is used in our analysis. From Table 1, we can see that the best fit value of parameter α has different symbols with different matter densities, and a more stringent constraint on parameters is given by the latter one. Furthermore, it should be noted that for the theoretical constraint on parameter α from sound speed of GCG fluid, it requires $0 \leq \alpha \leq 1$. Then the confidence regions for parameter α in figures should be cut off by this constraint.

Furthermore, we consider a case where the constructed total χ^2 expression is independent of $\Omega_{\rm m}$. The total χ^2 is expressed as

$$\chi^2_{\rm total}=\chi^2_{\rm SNIa}+\chi^2_{\rm OHD}+\chi^2_{\rm BAO_{D_V}}. \qquad (5)$$

For this case, the constraint result is shown in Fig. 2(a) and Table 2. It can be seen that though we do not consider a possible expression of matter density in the unified model of dark matter and dark energy, the constraint on GCG model parameters is very weak. Thus we have to discuss another constraint on GCG model including the high redshift CMB data. Considering that the uncertainties of $z_{\rm d}$ and z_* are only about 0.1% for the variable of matter density, here we take z_* and $z_{\rm d}$ as constants, and their values are $z_*=1090.51$, $z_{\rm d}=1020.50$ according to five-year WMAP. Using a distance-measurement quantity $l_{\rm A}$, for CMB constraint the χ^2 is constructed, $\chi^2_{{\rm CMB}_{l_{\rm A}}}(p_{\rm s})=[l_{\rm A}(p_{\rm s})-l_{\rm A_{obs}}]^2/\sigma^2_{l_{A_{\rm obs}}}$. We combine this χ^2 expression with others, and the total χ^2 can be written as

$$\chi^2_{\rm total}=\chi^2_{\rm SNIa}+\chi^2_{\rm OHD}+\chi^2_{\rm BAO}+\chi^2_{{\rm CMB}_{l_{\rm A}}}. \qquad (6)$$

The constraint result for this case is given in Fig. 2(a) and Table 2. From Table 2 we can see that the best fit value of parameter, $\alpha=0036$, is near to zero (for $\alpha=0$ the GCG model is reduced to ΛCDM), and this constraint on parameter α is stricter than the former case, but the confidence level is a little wide still. Therefore, we expect that the more stringent constraint on the unified model can be given by using more datapoints obtained from the cosmological distance measurement in the future, i.e., more observed datapoints or more exact data, which are independent of the

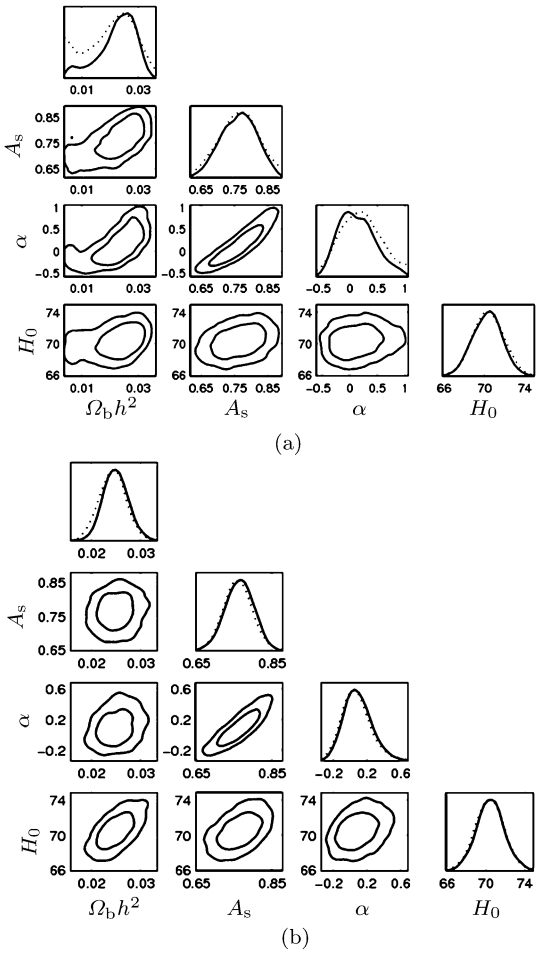


Fig. 2. The 1D constraints on individual parameters: $\Omega_{\rm b}h^2$, $A_{\rm s}$, α, H_0 and 2D contours on these parameters with 1σ and 2σ confidence levels between each other, where the total χ^2 expressions are given by Eqs. (5) (a) and (6) (b), respectively.

Table 2. The data fitting results of GCG model parameters with 1σ and 2σ confidence levels.

Parameter	SNIa + OHD + BAO$_{D_V}$	SNIa + OHD + BAO + CMB$_{l_A}$
$\Omega_b h^2$	$0.0262^{+0.0069+0.0091}_{-0.0211-0.0212}$	$0.0245^{+0.0052+0.0071}_{-0.0054-0.0065}$
A_s	$0.772^{+0.087+0.109}_{-0.118-0.140}$	$0.759^{+0.075+0.100}_{-0.077-0.100}$
α	$0.140^{+0.704+0.857}_{-0.520-0.678}$	$0.036^{+0.362+0.543}_{-0.250-0.329}$
H_0	$70.35^{+2.54+3.61}_{-2.50-3.64}$	$70.45^{+2.86+4.04}_{-3.04-4.08}$
$\chi^2_{min}(\chi^2_{min}/dof)$	476.969(1.155)	477.191(1.150)

For these two constraints, we do not assume an effective expression of matter density.

dynamical quantity Ω_m, can be utilized to constrain the GCG mixture. Thus, one can more exactly explore the possible interaction between the dark sections without considering any prior form of matter density. According to this constraint, one can rationally split the dark components in the unified model to investigate the possible evolution of dark energy. Finally, in Tables 1 and 2, we also calculate the value of χ^2_{min}/dof, where the value of dof for a model equals the number of observational data points minus the number of parameters.

4. Conclusion

The constraints on the unified model of dark matter and dark energy have been studied in this paper by using recently observed data: the Constitution dataset including 397 SNIa, the observational Hubble data, the baryon acoustic oscillation data and the five-year WMAP data. For this unified model, since the matter density parameter is not explicitly included in the background equation, we constrain the GCG model parameters by taking the effective expressions of matter density or considering the observed quantities that are independent of the matter density. The constraint results are listed in Tables 1 and 2. From Tables 1 and 2, we can see that the constraints on baryon matter density in GCG model are consistent with other constraints.[22] One knows that model parameter A_s denotes the current equation of state of GCG fluid. For the constraints on this parameter A_s, it is clearly to seen that the best fit value of A_s for the different constraints is much closer to each other. For parameter α, it is much more sensitive to the difference of constraints, and the most stringent constraint on this parameter is, $\alpha = 0.028^{+0.062}_{-0.049}(1\sigma)^{+0.087}_{-0.070}(2\sigma)$. However, if we consider the cosmological constraint being independent of the dynamical quantity Ω_m, the constraints on the GCG model parameters are a little relaxed. We expect that the more stringent constraint on the unified model can be given by using more datapoints or more exact data that will be obtained from the cosmological distance measurement in the future. Thus, one can more exactly explore the possible interactions between the dark sections and the evolution of dark energy without considering any prior situation on matter density.

Appendix A: Cosmological constraint methods and dataset

In this part, we introduce the cosmological constraints methods and the recently observed data used in this paper.

1) Type Ia supernovae

For SNIa measurement, we use the Constitution dataset[18] including 397 SNIa to constrain the cosmological parameters. This dataset is obtained by adding 90 SNIa from CfA3 sample to 307 SNIa Union sample.[30] CfA3 samples are all from the scope of redshift, $z < 0.08$, and these 90 SNIa are calculated by using the same Union cuts. This increases the low-redshift samples ($z \leq 0.2$) to 147 SNIa in the resulting Constitution dataset (The 307 SNIa union samples include 250 high-redshift SNIa ($z > 0.2$) and 57 low-redshift SNIa ($z \leq 0.2$) samples). With the addition of the nearby SNIa number it reduces the statistical uncertainties. Following Refs. [31] and [32], one can obtain the corresponding constraints by fitting the distance modulus $\mu(z)$ as

$$\mu_{th}(z) = 5\lg[D_L(z)] + \mu_0, \tag{A1}$$

where $D_L(z)$ is the Hubble-free luminosity distance with $D_L(z) = H_0 d_L(z)/c$, and

$$d_L(z) = c(1+z)\int_0^z \frac{dz'}{H(z')},$$
$$\mu_0 \equiv 42.38 - 5\lg h.$$

Additionally, the observed distance modulius $\mu_{\rm obs}(z_i)$ of SNIa at z_i is

$$\mu_{\rm obs}(z_i) = m_{\rm obs}(z_i) - M, \tag{A2}$$

where M is the absolute magnitude.

For the SNIa dataset, the best fit values of the parameters $p_{\rm s}$ can be determined by a likelihood analysis, based on the calculation of

$$\begin{aligned}&\chi^2({\rm p_s}, M')\\ \equiv &\sum_{\rm SNIa}\frac{\{\mu_{\rm obs}(z_i)-\mu_{\rm th}(p_{\rm s},z_i)\}^2}{\sigma_i^2}\\ = &\sum_{\rm SNIa}\frac{\{5\lg[D_{\rm L}(p_{\rm s},z_i)]-m_{\rm obs}(z_i)+M'\}^2}{\sigma_i^2},\end{aligned} \tag{A3}$$

where $p_{\rm s}$ denotes the parameters contained in the model, $M' \equiv \mu_0 + M$ is a nuisance parameter which includes the absolute magnitude and the parameter h. The nuisance parameter M' can be marginalized over analytically as[33,34]

$$\bar{\chi}^2(p_{\rm s}) = -2\ln\int_{-\infty}^{\infty}\exp\left[-\frac{1}{2}\chi^2(p_{\rm s},M')\right]{\rm d}M',$$

resulting in

$$\bar{\chi}^2 = A - \frac{B^2}{C} + \ln\left(\frac{C}{2\pi}\right), \tag{A4}$$

with

$$\begin{aligned}A &= \sum_{\rm SNIa}\frac{\{5\lg[D_L(p_{\rm s},z_i)]-m_{\rm obs}(z_i)\}^2}{\sigma_i^2},\\ B &= \sum_{\rm SNIa}\frac{5\lg[D_L(p_{\rm s},z_i)]-m_{\rm obs}(z_i)}{\sigma_i^2},\\ C &= \sum_{\rm SNIa}\frac{1}{\sigma_i^2}.\end{aligned}$$

Relation (A3) has a minimum at the nuisance parameter value $M' = B/C$, which contains information of the values of h and M. Therefore, one can extract the values of h and M provided that we know one of them. Finally, note that the expression

$$\chi^2_{\rm SNIa}(p_{\rm s}, B/C) = A - (B^2/C), \tag{A5}$$

which coincides with (A4) up to a constant, is often used in the likelihood analysis,[31,33] and thus in this case the results will not be affected by a flat M' distribution.

2) Observational Hubble data

The observational Hubble data[35,36] are based on differential ages of the galaxies. In Ref. [37], Jimenez *et al.* obtained an independent estimate for the Hubble parameter using the method developed in Ref. [38], and used it to constrain the dark energy models. The Hubble parameter, depending on the differential ages as a function of redshift z, can be written in the form of

$$H(z) = -\frac{1}{1+z}\frac{{\rm d}z}{{\rm d}t}. \tag{A6}$$

Hence, once ${\rm d}z/{\rm d}t$ is known, $H(z)$ can be obtained directly[19] By using the differential ages of passively evolving galaxies from the Gemini deep deep survey (GDDS)[39] and archival data,[40−45] Simon *et al.* obtained $H(z)$ in the range of $0 \le z \le 1.8$.[19] The twelve observational Hubble data from Refs. [46] and [47] are listed in Table A1. In addition, in Ref. [48] the authors took the BAO scale as a standard ruler in the radial direction, and obtained three more additional data: $H(z=0.24) = 79.69\pm2.32$, $H(z=0.34) = 83.8\pm2.96$, and $H(z=0.43) = 86.45 \pm 3.27$.

The best fit values of the model parameters from observational Hubble data are determined by minimizing[49]

$$\chi^2_{\rm OHD}(p_{\rm s}) = \sum_{i=1}^{15}\frac{[H_{\rm th}(p_{\rm s};z_i)-H_{\rm obs}(z_i)]^2}{\sigma^2(z_i)}, \tag{A7}$$

where $H_{\rm th}$ is the predicted value for the Hubble parameter, $H_{\rm obs}$ is the observed value, $\sigma(z_i)$ is the standard deviation measurement uncertainty, and the summation is over the 15 observational Hubble data points at redshifts z_i.

3) Baryon acoustic oscillation

The baryon acoustic oscillations are detected in the clustering of the combined 2dFGRS and SDSS main galaxy samples, and the distance-redshift relations are measured at $z = 0.2$ and $z = 0.35$. The observed scale of the BAO calculated from these samples, as well as from the combined sample, are jointly analysed using estimates of the correlated errors to constrain the form of the distance measure $D_{\rm V}(z)$[21,50]

$$D_{\rm V}(z) = \left[(1+z)^2 D_{\rm A}^2(z)\frac{cz}{H(z)}\right]^{1/3}. \tag{A8}$$

In this expression, $D_{\rm A}(z)$ is the proper (not comoving) angular diameter distance, which has the following relation with $d_{\rm L}(z)$:

$$D_{\rm A}(z) = \frac{d_{\rm L}(z)}{(1+z)^2}.$$

Table A1. The observational $H(z)$ data.[46,47]

z	0	0.1	0.17	0.27	0.4	0.48	0.88	0.9	1.30	1.43	1.53	1.75
$H(z)/\mathrm{km\cdot s^{-1}\cdot Mpc^{-1}}$	74.2	69	83	77	95	97	90	117	168	177	140	202
1σ uncertainty	±3.6	±12	±8	±14	±17	±60	±40	±23	±17	±18	±14	±40

The peak positions of the BAO depend on the ratio of $D_{\rm V}(z)$ to the sound horizon size at the drag epoch (where baryons were released from photons) $z_{\rm d}$, which can be obtained by using a fitting formula[51]

$$z_{\rm d}=\frac{1291(\Omega_{\rm m}h^2)^{-0.419}}{1+0.659(\Omega_{\rm m}h^2)^{0.828}}[1+b_1(\Omega_{\rm b}h^2)^{b_2}], \quad \text{(A9)}$$

with

$$b_1=0.313(\Omega_{\rm m}h^2)^{-0.419}[1+0.607(\Omega_{\rm m}h^2)^{0.674}], \quad \text{(A10)}$$

$$b_2=0.238(\Omega_{\rm m}h^2)^{0.223}. \quad \text{(A11)}$$

In this paper, we use the data of $r_{\rm s}(z_{\rm d})/D_{\rm V}(z)$ extracted from the SDSS and the 2dFGRS[52] which are listed in Table A2, where $r_{\rm s}(z)$ is the comoving sound horizon size

$$r_{\rm s}=c\int_0^t\frac{c_{\rm s}{\rm d}t}{a}=c\int_0^a\frac{c_{\rm s}{\rm d}a}{a^2H}=c\int_z^\infty{\rm d}z\frac{c_{\rm s}}{H(z)}$$
$$=\frac{c}{\sqrt{3}}\int_0^{1/(1+z)}\frac{{\rm d}a}{a^2H(a)\sqrt{1+(3\Omega_{\rm b}/(4\Omega_{\rm r})a)}}, \quad \text{(A12)}$$

where $c_{\rm s}$ is the sound speed of the photon–baryon fluid[53,54]

$$c_{\rm s}^{-2}=3+\frac{4}{3}\times\frac{\rho_{\rm b}(z)}{\rho_{\rm r}(z)}=3+\frac{4}{3}\times\left(\frac{\Omega_{\rm b}}{\Omega_{\rm r}}\right)a, \quad \text{(A13)}$$

and $\Omega_{\rm r}=2.469\times10^{-5}h^{-2}$ for $\mathrm{T_{CMB}}=2725$ K.

Table A2. The observational $r_{\rm s}(z_{\rm d})/D_{\rm V}(z)$ data.[21]

Z	$r_{\rm s}(z_{\rm d})/D_{\rm V}(z)$
0.2	0.1905 ± 0.0061
0.35	0.1097 ± 0.0036

Using the data of BAO in Table A2 and the inverse covariance matrix $\boldsymbol{V}^{-1}$ in Ref. [21]

$$\boldsymbol{V}^{-1}=\begin{pmatrix}30124.1 & -17226.9\\ -17226.9 & 86976.6\end{pmatrix}; \quad \text{(A14)}$$

the $\chi^2_{\rm BAO}(p_{\rm s})$ is given as

$$\chi^2_{\rm BAO}(p_{\rm s})=\boldsymbol{X}^{\rm t}\boldsymbol{V}^{-1}\boldsymbol{X}, \quad \text{(A15)}$$

where $\boldsymbol{X}$ is a column vector formed from the theoretical values minus the corresponding observational data, with

$$\boldsymbol{X}=\begin{pmatrix}\dfrac{r_{\rm s}(z_{\rm d})}{D_{\rm V}(0.2)}-0.190533\\ \dfrac{r_{\rm s}(z_{\rm d})}{D_{\rm V}(0.35)}-0.109715\end{pmatrix}, \quad \text{(A16)}$$

and $\boldsymbol{X}^{\rm t}$ denotes its transpose.

In addition, for BAO constraints a different χ^2 expression from the above one is also often used. Matching the BAO to have the same measured scale at all redshifts then gives an almost independent constraint on the ratio of distances[21]

$$D_{\rm V}(0.35)/D_{\rm V}(0.2)=1.736\pm0.065. \quad \text{(A17)}$$

The χ^2 expression for using this quantity to constrain the cosmological models can be given as

$$\chi^2_{{\rm BAO}_{D_{\rm V}}}(p_{\rm s})=\frac{[D_{\rm V}(0.35)/D_{\rm V}(0.2)-1.736]^2}{0.065^2}, \quad \text{(A18)}$$

which is independent of the matter density.

4) Cosmic microwave background

Table A3. The values of $l_{\rm A}(z_*), R(z_*)$, and z_* from 5-year WMAP result.

	5-year maximum likelihood	error (σ)
$l_{\rm A}(z_*)$	302.10	0.86
$R(z_*)$	1.710	0.019
z_*	1090.04	0.93

Table A4. The inverse covariance matrix of $\mathrm{l_A}(z_*), \mathrm{R}(z_*)$, and z_* from 5-year WMAP data.

	$l_{\rm A}(z_*)$	$R(z_*)$	z_*
$l_{\rm A}(z_*)$	1.8000	27.968	−1.103
$R(z_*)$		5667.577	−92.263
z_*			2.923

The CMB shift parameter R is provided by[54]

$$R(z_*)=\sqrt{\Omega_{\rm m}H_0^2}(1+z_*)D_{\rm A}(z_*)/c, \quad \text{(A19)}$$

which is related to the second distance ratio $D_{\rm A}(z_*)H(z_*)/c$ by a factor $\sqrt{1+z_*}$. The redshift z_* (the decoupling epoch of photons) is obtained using the fitting function[55]

$$z_*=1048[1+0.00124(\Omega_{\rm b}h^2)^{-0.738}][1+g_1(\Omega_{\rm m}h^2)^{g_2}],$$

where the functions g_1 and g_2 read

$$g_1 = 0.0783(\Omega_{\rm b}h^2)^{-0.238}(1+39.5(\Omega_{\rm b}h^2)^{0.763})^{-1},$$
$$g_2 = 0.560(1+21.1(\Omega_{\rm b}h^2)^{1.81})^{-1}.$$

In additional, the acoustic scale is related to the first distance ratio, $D_{\rm A}(z_*)/r_{\rm s}(z_*)$, and the angular scale of the sound horizon at decoupling epoch is defined as

$$l_{\rm A} \equiv (1+z_*)\frac{\pi D_{\rm A}(z_*)}{r_{\rm s}(z_*)}. \tag{A20}$$

where a factor of $1+z_*$ arises because $D_{\rm A}(z)$ is the proper (physical) angular diameter distance, whereas $r_{\rm s}(z_*)$ is the comoving sound horizon at z_*. Using the data of $l_{\rm A}, R, z_*$ in Ref. [22] and their covariance matrix of $[l_{\rm A}(z_*), R(z_*), z_*]$ (see Table A3 and A4), we can calculate the likelihood L as $\chi^2_{\rm CMB} = -2\ln L$

$$\chi^2_{\rm CMB} = \Delta \boldsymbol{d}_i[{\rm Cov}^{-1}(\boldsymbol{d}_i, \boldsymbol{d}_j)[\Delta \boldsymbol{d}_i]^t], \tag{A21}$$

where $\Delta \boldsymbol{d}_i = \boldsymbol{d}_i - \boldsymbol{d}_i^{\rm data}$ is a row vector, and $\boldsymbol{d}_i = (l_{\rm A}, R, z_*)$.

References

[1] Riess A G, Filippenko A V, Challis P, Clocchiattia A, Diercks A, Garnavich P M, Gilliland R L, Hogan C J, Jha S, Kirshner R P, Leibundgut B, Phillips M M, Reiss D, Schmidt B P, Schommer R A, Smith R C, Spyromilio J, Stubbs C, Suntzeff N B and Tonry J 1998 *Astron. J.* **116** 1009

[2] Spergel D N, Verde L, Peiris H V, Komatsu E, Nolta M R, Bennett C L, Halpern M, Hinshaw G, Jarosik N, Kogut A, Limon M, Meyer S S, Page L, Tucker G S, Weiland J L, Wollack E and Wright E L 2003 *Astrophys. J. Suppl.* **148** 175

[3] Pope A C, Matsubara T, Szalay A S, Blanton M R, Eisenstein D J, Gray J, Jain B, Bahcall N A, Brinkmann J, Budavari T, Connolly A J, Frieman J A, Gunn J E, Johnston D, Kent S M, Lupton R H, Meiksin A, Nichol R C, Schneider D P, Scranton R, Strauss M A, Szapudi I, Tegmark M, Vogeley M S, Weinberg D H and Zehavi I 2004 *Astrophys. J.* **607** 655

[4] Weinberg S 1989 *Mod. Phys. Rev.* **61** 527

[5] Zhai X H and Zhao Y B 2006 *Chin. Phys.* **15** 10

[6] Zhao W 2007 *Chin. Phys.* **16** 9

[7] Feng B, Wang X L and Zhang X M 2005 *Phys. Lett.* B **607** 35

[8] Lu J B, Saridakis E N, Setare M R and Xu L X 2010 *JCAP* **03** 031

[9] Li M 2004 *Phys. Lett.* B **603** 1

[10] Gong Y G 2005 *Class. Quant. Grav.* **22** 2121

[11] Wu Y B, Lu J B, He J and Fu M H 2007 *Chin. Phys.* **16** 20

[12] Zhu Z H and Alcaniz J S 2005 *Astrophys. J.* **620** 7

[13] Liu M L, Liu H Y, Zhang J F and Yu F 2008 *Chin. Phys.* B **17** 5

[14] Kamenshchik A Y, Moschella U and Pasquier V 2001 *Phys. Lett.* B **511** 265

[15] Bento M C, Bertolami O and Sen A A. 2002 *Phys. Rev.* D **66** 043507

[16] Zhu Z H 2004 *Astron. Astrophys.* **423** 421

[17] Lu J B, Xu L X, Li J C, Chang B R, Gui Y X and Liu H Y 2008 *Phys. Lett.* B **662** 87

[18] Hicken M 2009 *Astrophys. J.* **700** 1097

[19] Simon J, Verde L and Jimenez R 2005 *Phys. Rev.* D **71** 123001

[20] Eisenstein D J, Zehavi I, Hogg D W, *et al.* 2005 *Astrophys. J.* **633** 560

[21] Percival W J, Reid B A and Eisenstein D J 2010 *Mon, Not. Roy. Astron. Soc.* **401** 2148

[22] Komatsu E 2009 *Astrophys. J. Suppl.* **180** 330

[23] Lewis A and Bridle S 2002 *Phys. Rev.* D **66** 103511

[24] Makler M, Oliveira S Q and Waga I 2003 *Phys. Rev.* D **68** 123521

[25] Zhu Z H 2004 *Astron. Astrophys.* **423** 421

[26] Wu P X and Yu H W 2007 *Phys. Lett.* B **644** 16

[27] Silva P T and Bertolami O 2003 *Astrophys. J.* **599** 829

[28] Bento M C, Bertolami O and Sen A A 2003 *Phys. Lett.* B **575** 172

[29] Li M, Li X D and Zhang X 2010 *Sci. China.* Ser. G **53** 1631

[30] Kowalski M 2008 *ApJ* **686** 749

[31] Gong Y G, Wang B and Cai R G 2010 *JCAP* **04** 019

[32] Gannouji R and Polarski D 2008 *JCAP* **05** 018

[33] Nesseris S and Perivolaropoulos L 2005 *Phys. Rev.* D **72** 123519

[34] Lu J B 2009 *Phys. Lett.* B **680** 404

[35] Yi Z L and Zhang T J 2007 *Mod. Phys. Lett.* A **22** 41

[36] Zhai Z X, Wan H Y and Zhang T J 2010 *Phys. Lett.* B **689** 8

[37] Jimenez R, Verde L, Treu T and Stern D 2003 *Astrophys. J.* **593** 622

[38] Jimenez R and Loeb A 2002 *Astrophys. J.* **573** 37

[39] Abraham R G 2004 *Astron. J.* **127** 2455

[40] Treu T, Stiavelli M, Casertano S, Moller P and Bertin G 1999 *Mon. Not. Roy. Astron. Soc.* **308** 1037

[41] Treu T, Stiavelli M, Moller P, Casertano S and Bertin G 2001 *Mon. Not. Roy. Astron. Soc.* **326** 221

[42] Treu T, Stiavelli M, Moller P, Casertano S and Bertin G 2002 *Astrophys. J. Lett.* **564** L13

[43] Dunlop J, Peacock J, Spinrad H, Dey A, Jimenez R, Stern D and Windhorst R 1996 *Nature* **381** 581

[44] Spinrad H, Dey A, Stern D, Dunlop J, Peacock J, Jimenez R and Windhorst R 1997 *Astrophys. J.* **484** 581

[45] Nolan L A, Dunlop J S, Jimenez R and Heavens A F 2003 *Mon. Not. Roy. Astron. Soc.* **341** 464

[46] Riess A G 2009 *Astrophys. J.* **699** 539

[47] Stern D arXiv:0907.3149 [astro-ph.CO]

[48] Gaztanaga E arXiv:0807.3551 [astro-ph.CO]

[49] Lazkoz R and Majerotto E 2007 *JCAP* **07** 015

[50] Percival W J 2007 *Mon. Not. Roy. Astron. Soc.* **381** 1053

[51] Eisenstein D J and Hu W 1998 *Astrophys. J.* **496** 605

[52] Hu W and Sugiyama N 1995 *Astrophys. J.* **444** 489

[53] Hu W, Fukugita M, Zaldarriaga M and Tegmark M 2001 *Astrophys. J.* **549** 669

[54] Bond J R, Efstathiou G and Tegmark M 1997 *Mon. Not. Roy. Astron. Soc.* **291** L33

[55] Hu W and Sugiyama N 1996 *Astrophys. J.* **471** 542